



Chlorpyrifos fate in the Arctic: Importance of analyte structure in interactions with Arctic dissolved organic matter

Lauren E. O'Connor^a, Pippin Robison^b, Ginna Quesada^c, Jill F. Kerrigan^a, Robyn C. O'Halloran^a, Jennifer J. Guerard^{b,*}, Yu-Ping Chin^{a,*}

^a Department of Civil and Environmental Engineering, University of Delaware, 127 The Green, Newark, DE 19716, USA

^b Chemistry Department, United States Naval Academy, Annapolis, MD 21402, USA

^c Department of Chemistry and Biochemistry, University of Alaska Fairbanks, Fairbanks, AK 99775, USA

ARTICLE INFO

Keywords:

Dissolved organic matter
Arctic
Partitioning
Chlorpyrifos
Photochemistry

ABSTRACT

The insecticide and current use pesticide chlorpyrifos (CLP) is transported *via* global distillation to the Arctic where it may pose a threat to this ecosystem. CLP is readily detected in Arctic environmental compartments, but current research has not studied its partitioning between water and dissolved organic matter (DOM) nor the role of photochemistry in CLP's fate in aquatic systems. Here, the partition coefficients of CLP were quantified with various types of DOM isolated from the Arctic and an International Humic Substances Society (IHSS) reference material Suwannee River natural organic matter (SRNOM). While CLP readily partitions to DOM, CLP exhibits a significantly higher binding constant with Arctic lacustrine DOM relative to fluvial DOM or SRNOM. The experimental partitioning coefficients (K_{DOC}) were compared to a calculated value estimated using poly parameter linear free energy relationship (pp-LFER) and was found to be in good agreement with SRNOM, but none of the Arctic DOMs. We found that Arctic K_{DOC} values decrease with increasing SUVA₂₅₄, but no correlations were observed for the other DOM compositional parameters. DOM also mediates the photodegradation of CLP, with stark differences in photo-kinetics using Arctic DOM isolated over time and space. This work highlights the chemo-diversity of Arctic DOM relative to IHSS reference materials and highlights the need for in-depth characterization of DOM that transcends the current paradigm based upon terrestrial and microbial precursors.

1. Introduction

Current use pesticides (CUPs) are a class of chemicals that replaced legacy pesticides and have been detected in environmental compartments (air, water, biota, sediment) globally (Khairy et al. 2016, Hageman et al. 2019, Balmer et al. 2019, Iturburu et al. 2019; and references therein). Multiple studies provide evidence of CUPs persisting in the environment, bioaccumulating, and showing some degree of toxicity to various organisms (Huang et al., 2020; Cáceres et al., 2007). CUP usage has steadily increased due to agricultural applications and as a consequence, remote locations such as the Arctic have also experienced a higher incidence of detection of these compounds (Balmer et al., 2019). According to the Arctic Monitoring and Assessment Program (AMAP), CUPs have made the list of chemicals of emerging concern (AMAP, 2017).

Chlorpyrifos (CLP) is an organophosphate CUP that is widely applied to consumer crops (Balmer et al., 2019). Approximately 10 million

pounds of CLP are used annually, and studies show that this chemical is likely to volatilize, remain in the atmosphere, and be transported distally (Golla et al., 2012; Hageman et al., 2019). While it has recently been banned in the United States, it is still widely used elsewhere. As such, CLP has also been readily detected across the Arctic in sea ice, sea water, soil, sediment, and in lakes (Balmer et al., 2019).

Chemical partitioning to dissolved organic matter (DOM) is an important process that influences a chemical's fate in aquatic ecosystems (Chiou et al. 1986, Chin et al. 1997, Neale et al. 2011, Wei-Haas et al. 2014, Liu et al. 2019, 2020, Peña et al. 2022, Vitale et al. 2019 and references therein). CLP has multiple characteristics that make it partition to DOM, most notably its hydrophobicity as quantified by its high octanol-water partitioning coefficient. When CLP interacts with DOM, this can alter its bioavailability and transport within a freshwater system (Grannas et al., 2012; Akkanen et al., 2004; Uhle et al., 1999). Further, the interaction of CLP and DOM may influence its photo-fate, an important attenuation process in Arctic surface waters during the

* Corresponding authors.

E-mail addresses: guerard@usna.edu (J.J. Guerard), yochin@udel.edu (Y.-P. Chin).

ice-free summer season.

DOM is ubiquitous in aquatic environments and is unique to their specific geographic location. DOM is composed of a matrix of degraded carbon either being allochthonous or autochthonous, i.e., carbon from the watershed or from within the water source, respectively (Wei-Hass et al., 2014). DOM from Alaskan Arctic surface waters is composed of plant and soil precursors that creates a rich DOM environment found across the Arctic (Grannas et al., 2012). The variable DOM concentrations in Arctic surface waters makes the partition coefficient an important parameter to determine CLP's fate in Arctic surface waters. For example, in rivers and wetlands high in DOM, these complexes may shield organisms from the toxic effects of CLP, while photochemical production of reactive species from the irradiation of DOM could facilitate the transformation of CLP.

Single and poly parameter linear free energy relationships (sp-LFER and pp-LFER, respectively) have been used to predict the partitioning of organic molecules to DOM. sp-LFER is most often used, but is limited in its application because of its reliance on a single compound property such as the octanol-water partition coefficient (K_{ow}) (Burkhard, 2000). pp-LFERs conversely utilize multiple parameters that better define the solute and properties that characterize the partitioning system. Therefore, pp-LFER models better estimate the partitioning interaction between organic molecules and DOM.

We studied the partitioning between CLP and DOM using Arctic DOM isolated from various surface waters and Suwannee River natural organic matter (SRNOM), which is an International Humic Substances Society (IHSS) reference material. The solubility enhancement method was used to determine the partitioning coefficients for CLP. These values were compared to the calculated theoretical value (pp-LFER) using solute and DOM descriptors (Goss et al., 2001). We also characterized DOM spectroscopic properties to elucidate the possible moieties responsible for CLP-DOM partitioning. In addition, we also examined the role of DOM in mediating the photolysis of CLP.

2. Materials and methods

2.1. Site description

DOM samples were collected from four Arctic locations on the North Slope of the Brooks Range, Alaska: Toolik Lake (68.63°N 149.59°W), Fog 1 Lake (68.67°N 149.09°W), and two tundra seeps adjacent to the Sagavanirktok (Sag; 68.88°N , 148.87°W) and Oksrukuyik (Oks; 68.68°N , 149.13°W) rivers (Fig. S1). The area is characterized by continuous permafrost and tussock tundra vegetation (Cory et al., 2007). Toolik lake has both inlet and outlet streams that hydrologically connect it to the local watershed and receives a small, but relatively constant source of terrestrially derived DOM throughout the ice-free season. In contrast Fog 1 lacks any such hydrologic connection and can only receive allochthonous inputs through overland runoff. The seeps are dark water shallow groundwater seeps characterized by high DOC (Fig. S2 and Table S1). Details on sampling, chemicals utilized, and PPL extraction (Dittmar et al., 2008) are described in the Supplemental Information.

2.2. DOM isolation and characterization

DOM from each site was isolated using styrene-divinylbenzene (PPL) solid phase extraction (SPE) cartridges using the method of Dittmar et al. (2008). Briefly, 100 liters of filtered sample were acidified to pH 2 and passed across a PPL-SPE, dried, and eluted with methanol. The eluent was evaporated, reconstituted in $18.2\text{ M}\Omega$ water and lyophilized. Recovery rates averaged $\sim 60\%$ (Table S1). Dissolved organic carbon was quantified on a Shimadzu total organic carbon analyzer (TOC-L) as non-purgeable organic carbon, and elemental composition of DOM isolates was performed on a VarioEL CHNS elemental analyzer. DOM isolates were characterized by ^1H SPR-W5-WATERGATE (Lam and

Simpson, 2008) and ^{13}C multiCP-MAS (Johnson and Schmidt-Rohr, 2014) nuclear magnetic resonance (NMR). NMR spectra were acquired on a Bruker Advance III 600.16 MHz running TopSpin 4.0.7 as described previously (Gagne et al., 2020) and are described in more detail in the Supporting Information (Section S5). DOM absorbance and fluorescence excitation emission matrices (EEMs) were measured on a Horiba Scientific Aqualog according to methods in Wei-Hass et al. (2014). Specific methods and calculations of absorbance and fluorescence indices are described in more detail in the Supporting Information (Section S7).

2.3. Solubility enhancement experiments

DOM stock solutions were made using 100 mg C L^{-1} of PPL Arctic DOM isolate or SRNOM dissolved in $18.2\text{ M}\Omega$ water and filtered through pyrolyzed $0.7\text{ }\mu\text{m}$ GF/F filters. A 7 mM CLP stock in hexane was plated (excess up to 10x aqueous solubility) into 10 mL glass centrifuge vials and the solvent was allowed to evaporate until the hexane was no longer present ($\sim 1\text{--}2\text{ min}$). DOM stock, diluted with a KH_2PO_4 buffer (pH 5) to achieve $0\text{--}100\text{ mg C L}^{-1}$, were added to each vial to a final volume of 10 mL . Vials were capped with aluminum foil to avoid sorption to the Teflon cap, placed in the dark and equilibrated for 7 days at 25°C with constant agitation. Kinetics experiments were conducted to determine the minimum time needed to reach equilibrium (Fig. S3). Once equilibration was reached, vials were centrifuged for 10 min at 112 rcf and CLP was quantified by HPLC (Shimadzu Nexera-i LC-2040C 3D; 15 cm Pinnacle II C18 Restek column, 15% H_3PO_4 : 85% CH_3OH v/v at 40°C), detected at 290 nm . Three separate solubility enhancement experiments were run each with triplicate vials at every DOC concentration to determine a $\log K_{DOC}$ for each DOM isolate in this study, for a total sample size of 9 for each $\log K_{DOC}$ determination.

2.4. Determination of K_{DOC}

The K_{DOC} values (L kg^{-1}) were calculated from the solubility enhancement experiments using the equation (Chiou et al., 1986):

$$S_w^* / S_w = 1 + K_{DOC} [\text{DOC}] \quad (1)$$

where, S_w^* and S_w are the apparent solubility in the respective presence and absence of DOM. To estimate K_{DOC} we used a poly-parameter linear free energy relationship (Goss et al., 2001).

$$\log(K) = eE + sS + aA + bB + vV + c \quad (2)$$

where, the capital letters represent the solute descriptors while the lower-case letters represent the properties of the partitioning system (Goss et al., 2001). E is the excess molar refraction of CLP, A and B are the respective H donor-acceptor properties, and V is the molar volume of the compound.

For our model, solute descriptors from Stenzel et al. (2013) were developed based on retention times from gas chromatography mass spectrometry measurements. The authors gathered the retention times and partitioning coefficients for various "liquid/condensed phase systems". Once these were obtained for CLP, using Excel Solver descriptors S , B , A , and L were calculated and V was determined based on molecular structure. The DOM descriptors were obtained from Kipka and DiToro (2011) specifically for Suwannee River fulvic acid (Table S2).

2.5. Photolysis experiments

Stock solutions of CLP ($\sim 20\text{ mM}$) were prepared in methanol and $450\text{ }\mu\text{L}$ were plated inside 500 mL amber glass bottles, which were rotated to coat them with a thin film of the solution and left to evaporate for 24 h , to ensure saturation of CLP (5x aq. solubility) in solution. Either 300 mL (for DOM experiments) or 400 mL (for direct photolysis experiments) of pH adjusted $18.2\text{ M}\Omega$ water was added and left to equilibrate with the pesticide thin film for an average of 18 h , (kinetics tested

for time to reach equilibrium, data not shown). For DOM experiments, thin film solutions were transferred to a separate 500 mL amber media bottle and combined with pH adjusted DOM stock (50 mg C L⁻¹) to yield a final concentration of ~ 10 mg C L⁻¹ in the reaction solution.

10 mL quartz tubes (Robson Scientific; Hertfordshire, England) were filled with reaction solutions in a dark environment and sealed with Teflon lined screw caps. Dark controls were wrapped with aluminum foil. Each experiment was carried out in triplicate. Solutions were irradiated in a Suntest CPS+ (ATLAS; Mount Prospect, IL, USA) solar simulator equipped with a Xenon arc lamp (1500 W) set to 500 W/m², and monitored with a SolarLight PMA 2100 radiometer (Glenside, PA, USA). Irradiance was also monitored by p-nitroanisole actinometry (Dulin and Mill, 1982). All solutions were stored in the dark at 4 °C to minimize hydrolysis. CLP was quantified by high performance liquid chromatography (HPLC: either Agilent 1100 or 1200 series) in triplicate with a 150 mm Restek Ultra C18 reverse-phase column (5 µm particle size; 4 mm diameter) in acetonitrile:0.1% acetic acid (80:20% v/v) at a flow rate of 1 mL/min, detected at 290 nm and quantified against prepared and external standards. Select chemical probes to promote or inhibit reactive transients were also added to reaction solutions in the presence of Fog 1 and Toolik 21 Freshet DOM, and a subset of reaction solutions were extracted for product analysis. These methods and results are detailed in the Supporting Information (SI).

2.6. Statistical analysis and photodegradation kinetics

Rate constants were calculated from a least-squares fit of the triplicate degradation data to a pseudo-first-order kinetics model using GraphPad Prism v. 9.5.0 for all statistical analyses. For photolysis experiments, apparent rate coefficients (k_{obs}) were corrected (k_{corr}) for aggregate light screening factors (S_{\sum_i}) (Miller and Chin, 2002) and quantum yield was determined from photon flux and actinometry as described in the SI. Statistically significant differences between rate constants (k_{cor}), between log K_{DOC} values, and between pairs of variables were determined at a 95% confidence interval via a Student's two-tail t-test with Welch's correction (for different standard deviations). Associations between pairs of variables were tested with the Pearson correlation (r coefficient). Standard deviations are reported with all associated values.

3. Results

3.1. DOM site composition

Spatial, temporal, and geochemical differences exist across the different environments from which DOM is derived that may influence both partitioning and contaminant transformation processes (Guerard et al., 2009). We isolated DOM from two different Arctic lakes (Toolik and Fog 1), the inlet stream to Toolik Lake, and two different tundra meltwater seeps to capture the diversity of Arctic DOM composition on influencing CLP partitioning to DOM. To assess temporal variability, we utilized Toolik Lake and Oksrukuyik Seep DOM isolates collected over a period of 7 years and/or different points in the season.

The Arctic isolates display a wide range of characteristics. Dissolved organic carbon (DOC) concentrations ranged from as low as 3 mg C L⁻¹ in Fog 1 Lake to upwards of 15 mg C L⁻¹ in the meltwater seeps (Table S1). Specific conductivity and pH were similar across all sites, and percent recovery of DOM (as carbon) by the PPL isolation process was on average a little over 60%. Elemental composition for each DOM isolate is similar to the range reported for other Arctic and IHSS reference and standard DOMs (Cory et al., 2007). The Arctic DOM had lower C:N compared to SRNOM and may reflect a somewhat more autochthonous character of DOM in Arctic water bodies but is not as low as that reported for Pony Lake fulvic acid (PLFA).

UV-visible spectroscopy absorbance curves reflected typical spectra observed for all DOM, showing broad relatively featureless profiles with

decreases in absorbance with increasing wavelength. Specific absorbance at 254 nm (SUVA₂₅₄) ranged from 2.84 (PLFA) up to 4.95 (SRNOM) L mg C⁻¹ m⁻¹ while E2:E3 also showed variability, ranging from 5.12 to 7.47 (Table 1), and are similar to IHSS reference natural organic matter and reported literature values for a wide range of DOM derived globally (Wei-Haas et al., 2014; Cawley et al., 2013; Cory et al., 2010; Guerard et al., 2009).

Fluorescence EEMS (Fig. S6) were used to determine the humification index (HIX), biological index (BIX), and fluorescence index (FI). HIX did not vary greatly among samples while BIX and FI revealed greater variability that reflects differences in the composition of the DOM precursor materials. BIX, FI, and SUVA₂₅₄ values for SRNOM and PLFA reflect their respective biogeochemical end-member status with opposite BIX, SUVA, and FI values (Table 1). Our Arctic DOM samples had BIX, FI, and SUVA range that more resemble a material derived from a combination of organic matter (autochthonous and allochthonous) represented by these endmembers (Table 1).

Relative functional group composition varied across all DOM isolates. NMR spectra highlight broad features due to the diversity of signals within the DOM, but overall, are extremely similar across all Arctic samples (Fig. 1). Some individual peaks with enough resolution to see peak splitting can be observed in the proton spectra (Fig. S4), and the degree to which these are present does differ between samples, however they are not well resolved enough for identification. Solid state carbon spectra, however, reveal consistent broad features (including three distinct bumps in the aromatic region) for all Arctic samples.

Despite the visual similarity in the NMR spectra, relative abundances across functional group regions varies and, in some cases, widely. The DOM extracts with the greatest and lowest percent of molecules derived from linear terpenoids (MDLT; 0.6–1.6 ppm) are PLFA and SRFA, respectively, which are our biogeochemical endmembers (Table S3). Likewise, DOM isolates also bound the relative carbohydrate (3.2–4.5 ppm) and aromatic regions (¹H NMR: 6.5–8.4 ppm; ¹³C NMR: 90–160 ppm). The greatest and lowest percent composition of carboxyl rich alicyclic molecules (CRAMs) was observed in the PLFA and Toolik 19

Table 1

Composition and characterization of DOM isolates in this study for both above: optical indices and below: elemental composition. a. SRFA elemental composition from IHSS (IHSS, 2022). b. PLFA elemental composition from Cawley et al. (2013).

DOM Isolate	Fluorescence			Absorbance	
	FI	BIX	HIX	SUVA ₂₅₄ (L mg C ⁻¹ m ⁻¹)	E2:E3
Toolik 21 Freshet	1.39	0.52	0.95	4.09	5.31
Toolik 19 Mid (Jul)	1.42	0.62	0.93	3.25	6.79
Toolik 19 Early (May)	1.42	0.60	0.92	3.77	5.98
Toolik 13 Mid (Jul)	1.49	0.64	0.90	3.59	5.85
Fog 1 19	1.36	0.52	0.99	3.97	5.53
Oksrukuyik Seep 13	1.37	—	—	4.18	—
Oksrukuyik Seep 19	1.47	0.70	0.91	2.98	7.47
Sagavanirkto Seep 13	1.44	0.51	0.94	4.59	5.36
SRNOM (2R101N)	1.35	0.44	0.94	4.95	4.48
SRFA (1S101F)	1.30	0.48	1.02	3.81	5.37
PLFA (1R109F)	1.48	0.83	0.91	2.84	5.12
DOM Isolate	Elemental Composition				
	%N	%C	%S	C:N	C:H
Toolik 21 Freshet	1.07	57.24	0.67	53.74	10.93
Toolik 19 Mid (Jul)	1.26	57.25	0.85	45.32	17.39
Toolik 19 Early (May)	—	—	—	—	—
Toolik 13 Mid (Jul)	1.08	51.29	0.69	47.61	9.60
Fog 1 19	1.47	58.45	0.74	39.69	10.52
Oksrukuyik Seep 13	1.20	50.88	0.71	42.49	10.04
Oksrukuyik Seep 19	—	—	—	—	—
Sagavanirkto Seep 13	0.97	53.61	0.70	55.37	9.86
SRNOM (2R101N)	0.62	52.55	0.76	84.48	11.56
SRFA (1S101F) ^a	0.66	53.30	0.41	80.76	13.39
PLFA (1R109F) ^b	6.60	52.80	3.10	8.00	9.78

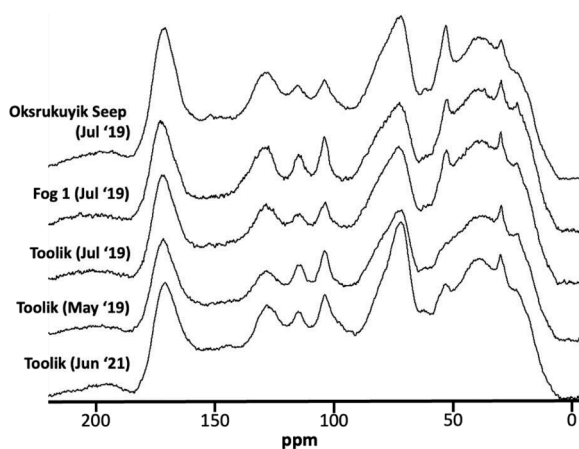


Fig. 1. Stacked ^{13}C multi-CP-MAS solid state NMR spectra of Arctic PPL DOM isolates.

Mid-Summer isolate, respectively. Arctic isolates with relatively high aromaticity include Toolik 21 freshet and Oksrukuyik Seep 19. Fog 1 isolate had a relatively low% aromaticity, similar to PLFA at 23.3%. Aliphatic to aromatic (Al:Ar) ratios also reflected these trends, with the summer Toolik isolates more in the middle of this range.

3.2. Partitioning coefficients of CLP to DOM

There is strong partitioning ($\log K_{\text{DOC}} > 3.5$) between CLP and DOM as determined by solubility enhancement (Fig. 2). Overall, solubility enhancement is linear with increasing DOC concentration (Fig. S5). Chlorpyrifos exhibits a relatively wide range of binding constants with Arctic DOM that span half an order of magnitude. The strongest partitioning was observed for Arctic lacustrine DOM isolates (Fig. 2). Toolik Lake (TL) isolates were all collected by PPL at differing points in the summer season (TL 21, spring freshet; TL19, early summer; TL13, mid-summer), but only TL13 differs in $\log K_{\text{DOC}}$ ($p = 0.01$) including from Fog 1, despite differences in SUVA₂₅₄ and other optical properties (Table 1). Chlorpyrifos preferentially partitions to lacustrine DOM relative to samples collected from fluvial and river seep derived DOM ($p = 0.02$), and preferentially partitions more strongly to *every* Arctic DOM isolate in this study compared to Suwannee River NOM ($p < 0.05$ for all DOMs vs. SR).

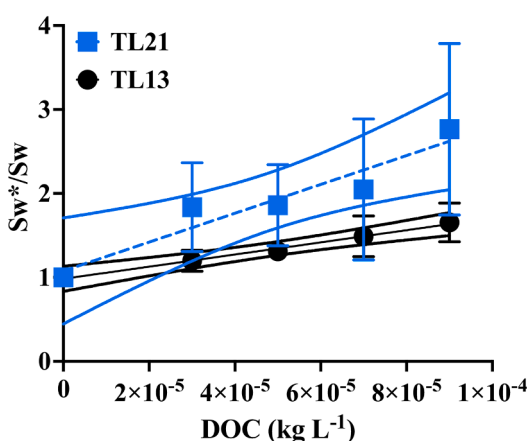


Fig. 2. Left: Solubility enhancement of chlorpyrifos to Toolik Lake (TL) 21 (blue) and TL 13 (orange) DOM. Right: $\log K_{\text{DOC}}$ of chlorpyrifos vs. DOM isolates. TL 21 spring freshet DOM; TL 19, 2013 and Fog Lake summer DOM; Sagavanirktoq R. (Sag) and Oksrukuyik Cr. (Oks) seep DOM; Suwannee R. (SR) DOM, pp-LFER. t-tests: $p < 0.05$ vs. a. TL 13; b. Sag; c. Oks; d. SR. Error bars represent standard deviations.

3.3. Comparing $\log K_{\text{DOC}}$ pp-LFER model and experimental results

The pp-LFER estimate for the $\log K_{\text{DOC}}$ for chlorpyrifos based on the system parameters derived from a generic pool of fulvic acids (Kipka and DiToro, 2011) is comparable to our experimentally derived value for SRNOM (< 0.2 log units, Fig. 2; Table S4). This is not surprising given that the system parameters for this pp-LFER model was derived from a training set, which includes Suwannee River fulvic acid (the most common DOM used in partitioning studies), which is compositionally similar to SRNOM (Kipka and DiToro, 2011). CLP K_{DOC} values for Arctic DOM, however, are all significantly higher by near an order of magnitude from the pp-LFER estimate. The pp-LFER descriptors accurately estimate CLP partitioning to the specific system (in our case SRNOM), but *cannot be universally applied* to DOM derived from other sources.

3.4. Photodegradation of CLP in the presence of DOM

CLP photodegraded rather slowly by direct photolysis, with a half-life ~ 17 h. Loss of CLP over time followed a pseudo-first order kinetic model (Fig. S7), with average R^2 values ~ 0.96 (Table S5). Overall, apparent quantum yields (AQYs) ranged from 6.23×10^{-5} to 2.28×10^{-4} (Table S5).

At circumneutral pH, nearly all isolates enhanced the photodegradation of CLP relative to direct photolysis (Fig. 3). The fastest rates of degradation were observed in the presence of Toolik19 early summer DOM isolate. The light screening corrected degradation rate constants

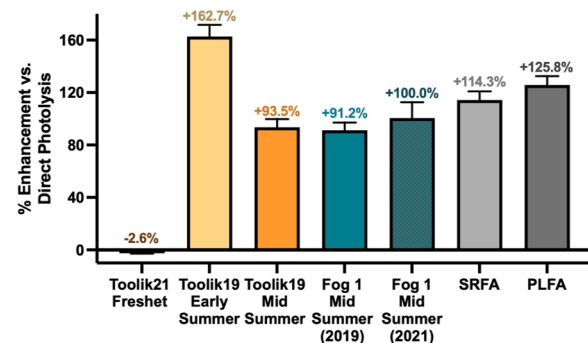
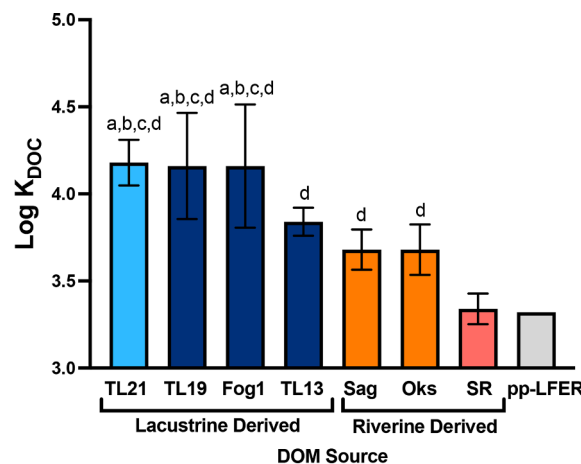


Fig. 3. Degree of enhancement in CLP pseudo-first order fitted rate constants corrected for light screening compared to that in ultrapure water (direct photolysis) in the presence of Arctic and IHSS DOM (SRFA = Suwannee River fulvic acid; PLFA = Pong Lake fulvic acid).



(k_{corr}) in the presence of SRFA, Fog 1, and Toolik19 Mid-Summer DOM were not statistically different from each other. Only one DOM isolate, Toolik 21 Freshet, did not significantly enhance the photodegradation of CLP (Fig. 3). Acidic (pH 5) and basic (pH 9) solution conditions resulted in some enhanced *direct* photodegradation relative to pH 7 and CLP degradation was enhanced by DOM relative to direct photolysis at high pH for all isolates tested (Fig. S8). No differences in the indirect photolysis rate constants of low pH solutions were observed in the presence of DOM except for Fog 1, which was the only DOM isolate where increased CLP degradation occurred under both low and high pH conditions. Results of CLP degradation in the presence of sensitizers and quenchers for specific mechanisms are described in Section S10.

3.5. Relationship between DOM character and CLP behavior

Linear regressions were performed between AQY, $\log K_{DOC}$, and DOM characterization properties (Table S6). $\log K_{DOC}$ was found to correlate positively with %C ($p = 0.01$), and negatively correlate with SUVA₂₅₄ ($p = 0.046$; Fig. 4). Other potential trends in relationship to $\log K_{DOC}$ may be E2:E3, percent aromaticity, and %S, which all had $R^2 > 0.4$ but $p > 0.05$, possibly due to low sample size (Fig. S10).

AQY derived from our photodegradation data did not significantly correlate to any parameters of DOM characterization: optical properties (FI, HIX, BIX, SUVA₂₅₄, E2:E3), NMR integrations, or elemental composition. While a significant correlation was found between AQY and $\log K_{DOC}$, the small sample size prevents interpretation as a significant conclusion. More studies are needed to test the significance of this relationship (Table S6). Despite SUVA₂₅₄ being typically correlated with aromaticity, no such trend in aromaticity and SUVA was found among the isolates in this study ($R^2 = 0.14$, $p = 0.32$, Fig. S10).

4. Discussion

4.1. Arctic DOM composition trends in seasonality and source

DOM has been isolated from Toolik Lake in a few prior studies over at least the last two decades, either using poly-methylmethacrylate resins (XAD-8) or by PPL solid phase extraction (Michaelson et al., 1998; Cory et al., 2007; Wei-Haas et al., 2014). These isolates have been typically characterized by optical fluorescence and absorbance, elemental composition, and NMR, though some studies have also investigated redox properties (Fimmen et al., 2007), photoreactivity (Cory et al., 2007; Ward and Cory, 2020), and association with contaminants (Grannas et al., 2012; Wei-Haas et al., 2014).

Toolik spring freshet waters ranged from 7 to 15 mg C L⁻¹ across three DOM extractions using different SPE resins from 1996 to 2021 (Michaelson et al. 1998, Cory et al. 2007; this study). XAD-8 extraction efficiencies ranged from 39 to 45% while PPL extraction efficiency are as

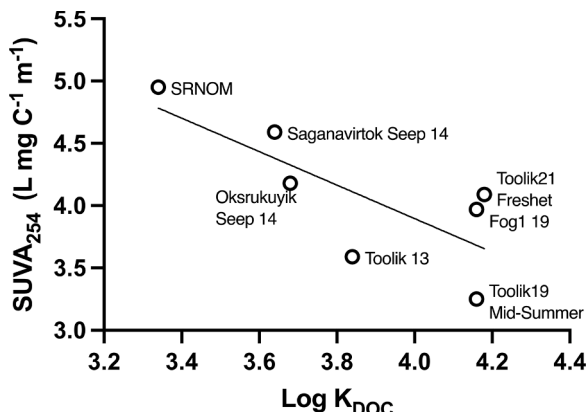


Fig. 4. Log K_{DOC} for chlorpyrifos vs. SUVA₂₅₄. $R^2 = 0.58$, $p = 0.046$.

high as 70.3%. Despite these differences in extraction method, FI of the isolate remained relatively similar (1.24 in 2003 from Cory et al., 2007 vs. 1.39 in 2021), as did the ¹³C NMR integrations (23.6% in 2003 from Cory et al. (2007) vs. 21.0% aromaticity as defined from 110 to 160 ppm), and elemental composition. For Toolik Lake summer isolations, there was more variability in extraction efficiency (15 and 34%, respectively, for XAD-8 in 1996 and 2002, and 60, 72, and 45% for PPL in 2013, 2019 May, and 2019 Jul). Despite that, FI varies only slightly (1.37 from Ward and Cory 2020 to 1.49 from Wei-Haas et al. 2014), and differences in SUVA₂₅₄ values are smaller (3.2–3.8 L mg C⁻¹ m⁻¹). Percent aromaticity was also relatively stable over these samplings, ranging from 17.7 to 19.1% (110–160 ppm). C:N differed more, with the largest C:N from the 2002 XAD-8 isolate (59.6 from Cory et al. 2007) and the lowest from 2019 mid-Summer (45.3). Overall, despite differences in the extraction method used, DOM isolates from Toolik Lake have remained considerably stable in chemical composition throughout its sampling history that has spanned a quarter century.

Arctic lacustrine waters are known to be oligotrophic, so presumably the DOM from these sources often exhibit allochthonous characteristics derived from terrestrial inputs (Cory et al., 2007). Toolik lake is thought to be ultraoligotrophic due to its low primary production rate (12 g carbon m⁻² y⁻¹). However, bacterial organic matter production was found to be 3–8 g carbon m⁻² y⁻¹ and makes up as much as 66% of the organic matter production in the pelagic zone (Crump et al., 2003). This high efficiency of bacterial production is associated with rapid bacterial growth and this process coupled with the production of “phytoplankton DOM” is the source of the autochthonous DOM (Crump et al., 2003). Regardless, DOM character over time and space can be altered as a result of the humification processes and our HIX values suggest our Arctic DOM has roughly undergone some degree of humification (Table 1).

Humic substances and other DOM components derived from terrestrial sources have been characterized as being more aromatic and possess higher SUVA₂₅₄, and lower FI (McKnight et al. 2001, Guerard et al. 2009, Cawley et al. 2013, Cory et al. 2007, Fimmen et al. 2007; and many others). The optical properties (FI, HIX, BIX, SUVA₂₅₄, and E2:E3) of our Arctic isolates fall within the range established for terrestrial and microbial DOM, which would suggest that the DOM in these lakes is sourced from a mix of both terrestrial and microbial sources. There is variability within the DOMs examined, however. For example, TL21 Freshet has nearly as high an aromaticity as SRNOM or SRFA, whereas Fog 1 DOM and Sagavanirkot Seep DOM both have low aromaticity and are similar to PLFA. Optical properties also reflect these trends, and suggest that Toolik 21 Freshet is more terrestrial in nature and Fog 1 DOM may be more microbial in composition, despite being separated by only 20 km.

Over the course of the summer season, aromatic content in the lacustrine DOM gradually decreases, from 21.1% down to 18.6%, which may indicate the incorporation of pelagic primary productivity components into the DOM pool. SUVA₂₅₄ also steadily declines from 4.09 down to 3.25 in isolates sampled as the season progressed and is also reflected in the higher N and S content in our DOM summer samples relative to spring freshet (TL21). Indeed, Fog 1 DOM has the highest N content, which may indicate the incorporation of pelagic biomass from primary producers over the course of the season. At the end of spring ice melt, there is a decrease in runoff from catchments which decreases the amount of terrestrial DOM inputs (Crump et al., 2003).

4.2. CLP sorption to Arctic DOM isolates

Despite the trends in seasonality with SUVA₂₅₄ decreasing over the summer season in Toolik Lake DOM isolates, there was a statistically significant negative relationship between $\log K_{DOC}$ for chlorpyrifos and SUVA₂₅₄ (Fig. 4) and yet a positive (though not significant) slope with aromaticity. SUVA₂₅₄ has historically correlated with aromaticity (Weishaar et al., 2003), however, the aromaticity of the DOM isolates in this study were not found to be correlated to SUVA₂₅₄ and if anything,

may suggest a negative relationship between these two (Fig. S10), suggesting the presence of other chromophores giving rise to absorbance e.g., ketones, metal complexes, etc. and potentially moieties that influence CLP sorption to Arctic DOM isolates.

In past studies, solubility enhancement experiments were conducted with legacy contaminants such as polychlorinated biphenyls, pesticides, and polycyclic aromatic hydrocarbons (Chiou et al., 1986; Chin et al., 1997; Uhle et al., 1999). These legacy contaminants are relatively simple in structure and their distribution in environmental compartments is largely dictated by their fugacity (Parnis and MacKay, 2020). While poly-parameter LFERs refined the simple fugacity and single parameter LFER models it cannot consider all solute and DOM specific properties. For example, ortho substitution of halogens in biphenyl-based compounds results in non-coplanar configurations that cause weaker partitioning and cannot be incorporated into pp-LFERs (Uhle et al., 1999). This difference in steric properties explains the large disparity in partitioning behavior to the same DOM for ortho substituted and co-planar PCB isomers.

Unlike many legacy contaminants, CLP possesses multiple regions of functionality: a phosphorus thionate with two non-rigid ethoxy groups, and a rigid chlorinated pyridine aromatic ring. While CLP's aromatic ring may provide potential for π - π stacking with aromatic moieties in the DOM, and favorable association of Arctic DOM with aromatic contaminants has been observed previously for hexachlorobenzene (HCB) (Grannas et al., 2012) and PDBEs (Wei-Haas et al., 2014), other analyte-DOM interactions are also important. Unfortunately, few data in the literature exist to compare log K_{DOC} values of chlorpyrifos. Neale et al. (2011) determined the log K_{DOC} for CLP and Aldrich humic acid to be 4.36 (\pm 0.12), which is surprisingly similar to the lacustrine K_{DOC} values reported here. Typically, the partitioning of hydrophobic analytes to commercial humic acids are significantly larger than aquatic derived DOM (Chin et al., 1997), and demonstrates that other interactions between CLP and Arctic DOM aside from aromaticity and hydrophobicity influence partitioning.

The pp-LFER only predicted log K_{DOC} reasonably well for the Arctic seep DOM samples and SRNOM. The reasonable estimates with respect to the latter is in large part due to the system parameters, which were derived from fulvic acid log K_{DOC} training sets (mostly Suwannee River fulvic acid). The much poorer pp-LFER estimates for the lacustrine DOM-CLP system again suggest that other interactions are responsible for our observations. While these solute and system poly-parameters considers some of the electron distribution through H-donor and acceptor interactions they cannot take into account other properties that might be unique to CLP functional groups such as phosphorous thionate. In addition, McGowan estimates of molar volumes does not consider the conformational flexibility of the larger ethoxy groups. Future work would benefit from chemical computational modeling of CLP with probe DOM surrogate molecules to study the potential binding dynamics with different moieties within CLP.

4.3. CLP photodegradation in Arctic DOM isolates

Unlike the summer Toolik and Fog 1 Lake DOMs, TL21, surprisingly, did not enhance photodegradation of CLP relative to direct photolysis. As their log K_{DOC} values are extremely similar to each other, this implies that photo-enhancement of CLP degradation may not entirely be a function of partitioning processes. Instead, this suggests that DOM composition differs enough to impact either the production and/or scavenging of reactive transients responsible for CLP photodegradation. Indeed, CLP degradation in TL21 DOM showed little change in degradation rates unless a sensitizer was added, whereas in Fog 1 DOM degradation seems to be potentially influenced by ROS (\bullet OH, 1 O₂; Fig. S9).

It is possible that TL21 DOM moieties act as efficient scavengers of produced reactive transients. DOM has been shown to inhibit photo-oxidative processes through its antioxidant properties (Wenk and

Canonica, 2012; Yang et al., 2022), however, SRFA which has been shown to have significant antioxidant moieties (Wenk and Canonica, 2012; Aeschbacher et al., 2012) did enhance CLP photodegradation. To better understand this process, it would be helpful to quantify these Arctic DOM isolates by their antioxidant properties (Wenk and Canonica, 2012; Aeschbacher et al., 2012). Insight into their electron donating and accepting capacity may better indicate the role of DOM in CLP photodegradation. CLP does oxidize, and is suspected to form the oxon (P=O) product in all photodegradation experiments, with the largest peak areas occurring in the presence of \bullet OH sensitizers, and smallest in the presence of \bullet OH scavengers (see Supporting Information S10).

Surprisingly, we observed no significant correlation between CLP AQY and DOM composition (Table S6). However, this may be due to the fact that CLP is potentially sensitive to multiple reactive transients, complicating its photochemistry with respect to DOM composition. The IHSS isolates, SRFA and PLFA, often thought of as endmembers of DOM reactivity and composition, based upon its fluorescent properties and aromaticity (Fig. S11), however, this simplified model did not explain DOM's role in the enhancement of CLP photodegradation. In fact, with respect to photoreactivity, Arctic DOMs over time and space possess higher variability than can be explained based upon precursor composition. Thus, a broad "allochthonous vs. autochthonous" comparison of DOM composition may not be specific enough for describing the functionalities that govern CLP interactions with DOM in general. In other studies, DOM properties and reactivity are no longer bound by the old paradigm based upon two biogeochemical endmembers (D'Andrilli et al., 2022; Gagné et al., 2023; Chin et al., 2023). CLP's partitioning and photoreactivity to Arctic DOM is a reflection of this new complex model of DOM.

5. Conclusion

Arctic DOM composition is remarkably stable in Toolik Lake on a scale of decades, and yet despite temporal stability over the long term, there are compositional shifts within a single season in DOM properties. Chlorpyrifos, a multifunctional molecule and emerging contaminant in the Arctic, provides a nuanced lens through which to observe the temporal and spatial compositional heterogeneity of Arctic DOM, through studying its sorption to DOM and its photochemical behavior. CLP partitioning to DOM is complicated, and potential interactions with DOM heteroatoms and conformational flexibility may cause predictive pp-LFER models to underestimate its partition coefficient. CLP photodegradation is also significantly enhanced in the presence of DOM, but does not correlate with any bulk compositional property of DOM. In summary, CLP may be a useful probe molecule to help better describe the multifaceted chemistry of DOM in aquatic environments.

Declaration of Competing Interest

The authors declare that they have no known competing financial interests or personal relationships that could have appeared to influence the work reported in this paper.

Data availability

Data will be made available on request.

Acknowledgments

This work was supported by NSF CBET-1804271 (Guerard) and NSF CBET-1804611 (Chin). This work was also supported by the United States Naval Academy (USNA) Trident and Bowman awards (Robison), Midshipman Research Support grant (Guerard), Department of Defense Threat Reduction Agency (Guerard), and NSF Graduate Research Fellowship (Quesada). Solution state NMR was run at the University of

Alaska Fairbanks Molecular Imaging Facility, which is in part supported by an Institutional Development Award (IDeA) from the National Institute of General Medical Sciences of the National Institutes of Health (P20GM103395). Thank you to A. Simpson for providing the SPR-W5-WATERGATE pulse sequence for the Bruker NMR. Thank you to the Toolik Field Station and staff for all of their support and help with sampling and field assistance, especially the Environmental Data Center. Thanks also to K Hageman and J Perala-Dewey for their field and laboratory assistance, and G Chateauneuf and M Schroeder for laboratory assistance.

Supplementary materials

Supplementary material associated with this article can be found, in the online version, at [doi:10.1016/j.watres.2023.120154](https://doi.org/10.1016/j.watres.2023.120154).

References

Aeschbacher, M., Graf, C., Schwarzenbach, R.P., Sander, M., 2012. Antioxidant properties of humic substances. *Environ. Sci. Technol.* 46 (9), 4916–4925. <https://doi.org/10.1021/es300039h>.

Akkonen, J., Vogt, R.D., Kukkonen, J.V.K., 2004. Essential characteristics of natural dissolved organic matter affecting the sorption of hydrophobic organic contaminants. *Aquat. Sci.* 66 (2), 171–177. <https://doi.org/10.1007/s00027-004-0705-x>.

AMAP, 2016. AMAP assessment. In: *Chemicals of Emerging Arctic Concern*, 2017. Arctic Monitoring and Assessment Programme (AMAP), Oslo, Norway, p. 353.

Balmer, J.E., Morris, A.D., Hung, H., Jantunen, L., Vorkamp, K., Rigét, F., Evans, M., Houde, M., Muir, D.C.G., 2019. Levels and trends of current-use pesticides (CUPs) in the Arctic: an updated review, 2010–2018. *Emerg. Contam.* (5), 70–88. <https://doi.org/10.1016/j.emcon.2019.02.002>.

Burkhard, L.P., 2000. Estimating dissolved organic carbon partition coefficients for nonionic organic chemicals. *Environ. Sci. Technol.* 34 (22), 4663–4668. <https://doi.org/10.1021/es001269l>.

Cáceres, T., He, W., Naidu, R., Megharaj, M., 2007. Toxicity of chlorpyrifos and TCP alone and in combination to daphnia carinata: the influence of microbial degradation in natural water. *Water Res.* 41 (19), 4497–4503. <https://doi.org/10.1016/j.watres.2007.06.025>.

Cawley, K.M., McKnight, D.M., Miller, P., Cory, R., Fimmen, R.L., Guerard, J., Dieser, M., Jaros, C., Chin, Y.P., Foreman, C., 2013. Characterization of fulvic acid fractions of dissolved organic matter during ice-out in a hyper-eutrophic, Coastal Pond in Antarctica. *Environm. Res. Lett.* 8 (4), 045015 <https://doi.org/10.1088/1748-9326/8/4/045015>.

Chin, Y.P., Aiken, G.R., Daniels, K.M., 1997. Binding of pyrene to aquatic and commercial humic substances: the role of molecular weight and aromaticity. *Environ. Sci. Technol.* 31 (6), 1630–1635.

Chin, Y.P., McKnight, D.M., D'Andrilli, J., Brooks, N., Cawley, K., Guerard, J., Perdue, E. M., Stedmon, C.A., Tratnyek, P.G., Westerhoff, P., Wozniak, A.S., Bloom, P.R., Foreman, C., Gabor, R., Hamdi, J., Hanson, B., Hozalski, R.M., Kellerman, A., McKay, G., Silverman, V., Spencer, R.G.M., Ward, C., Xin, D., Rosario-Ortiz, F., Remucal, C.K., Reckhow, D., 2023. Identification of next-generation international humic substances society reference materials for advancing the understanding of the role of natural organic matter in the anthropocene. *Aquat. Sci.* 85 (1), 32. <https://doi.org/10.1007/s00027-022-00923-x>.

Chiou, C.T., Malcolm, R.L., Brinton, T.I., Kile, D.E., 1986. Water solubility enhancement of some organic pollutants and pesticides by dissolved humic and fulvic acids. *Environ. Sci. Technol.* 20 (5), 502–508. <https://doi.org/10.1021/es00147a010>.

Cory, R.M., Miller, M.P., McKnight, D.M., Guerard, J.J., Miller, P.L., 2010. Effect of instrument-specific response on the analysis of fulvic acid fluorescence spectra. *Limnol. Oceanogr. Methods* 8 (2), 67–78. <https://doi.org/10.4319/lom.2010.8.67>.

Cory, R.M., McKnight, D.M., Chin, Y.P., Miller, P., Jaros, C.L., 2007. Chemical characteristics of fulvic acids from Arctic surface waters: microbial contributions and photochemical transformations. *J. Geophys. Res. Biogeosci.* 112 (G4) <https://doi.org/10.1029/2006JG000343>.

Crump, B.C., Kling, G.W., Bahr, M., Hobbie, J.E., 2003. Bacterioplankton community shifts in an Arctic Lake correlate with seasonal changes in organic matter source. *Appl. Environ. Microbiol.* 69 (4), 2253–2268. <https://doi.org/10.1128/AEM.69.4.2253-2268.2003>.

D'Andrilli, J., Silverman, V., Buckley, S., Rosario-Ortiz, F.L., 2022. Inferring ecosystem function from dissolved organic matter optical properties: a critical review. *Environ. Sci. Technol.* 56 (16), 11146–11161. <https://doi.org/10.1021/acest.2c04240>.

Dittmar, T., Koch, B., Hertkorn, N., Kattner, G., 2008. A simple and efficient method for the solid-phase extraction of dissolved organic matter (SPE-DOM) from seawater. *Limnol. Oceanogr. Methods* 6 (6), 230–235. <https://doi.org/10.4319/lom.2008.6.230>.

Dulin, D., Mill, T., 1982. Development and evaluation of sunlight actinometers. *Environ. Sci. Technol.* 16 (11), 815–820. <https://doi.org/10.1021/es00105a017>.

Fimmen, R.L., Cory, R.M., Chin, Y.P., Trout, T.D., McKnight, D.M., 2007. Probing the oxidation–reduction properties of terrestrially and microbially derived dissolved organic matter. *Geochim. Cosmochim. Acta* 71 (12), 3003–3015. <https://doi.org/10.1016/j.gca.2007.04.009>.

Gagné, K.R., Eckhardt, B.A., Walter Anthony, K.M., Barnes, D.L., Guerard, J.J., 2023. Dissolved organic matter from surface and pore waters of a discontinuous permafrost watershed in Central Alaska reveals both compositional and seasonal heterogeneity. *Aquat. Sci.* 85 (1), 31. <https://doi.org/10.1007/s00027-022-00930-y>.

Gagné, K.R., Ewers, S.C., Murphy, C.J., Daanen, R., Walter Anthony, K., Guerard, J.J., 2020. Permafrost organic matter characterization and chemical photoreactivity. *Environ. Sci. Processes Impacts* 22, 1525–1539. <https://doi.org/10.1039/d0em0097c>.

Golla, V., Curwin, B., Sanderson, W., Nishioka, M., 2012. Pesticide concentrations in vacuum dust from farm homes: variation between planting and nonplanting seasons. *ISRN Public Health* 2012, 1–10. <https://doi.org/10.5402/2012/539397>.

Grannas, A.M., Cory, R.M., Miller, P.L., Chin, Y.P., McKnight, D.M., 2012. The role of dissolved organic matter in Arctic surface waters in the photolysis of hexachlorobenzene and lindane. *J. Geophys. Res. Biogeosci.* 117 (G1) <https://doi.org/10.1029/2010JG001518>.

Goss, K.U., Schwarzenbach, R.P., 2001. Linear free energy relationships used to evaluate equilibrium partitioning of organic compounds. *Environ. Sci. Technol.* 35 (1), 1–9. <https://doi.org/10.1021/es000996d>.

Guerard, J.J., Miller, P.L., Trout, T.D., Chin, Y.P., 2009. The role of fulvic acid composition in the photosensitized degradation of aquatic contaminants. *Aquat. Sci.* 71 (2), 160–169. <https://doi.org/10.1007/s00027-009-9192-4>.

Hageman, K.J., Aebig, C.H.F., Luong, K.H., Kaserzon, S.L., Wong, C.S., Reeks, T., Greenwood, M., Macaulay, S., Matthaei, C.D., 2019. Current-use pesticides in New Zealand streams: comparing results from grab samples and three types of passive samplers. *Environ. Pollut.* 254, 112973 <https://doi.org/10.1016/j.envpol.2019.112973>.

Huang, X., Cui, H., Duan, W., 2020. Ecotoxicity of chlorpyrifos to aquatic organisms: a review. *Ecotoxicol. Environ. Saf.* 200, 110731 <https://doi.org/10.1016/j.ecoenv.2020.110731>.

IHSS, Elemental compositions and stable isotopic ratios of IHSS samples. 2022. <https:////humic-substances.org/elemental-compositions-and-stable-isotopic-ratios-of-ihs-samples/>.

Iturburu, F.G., Calderon, G., Amé, M.V., Menone, M.L., 2019. Ecological Risk Assessment (ERA) of pesticides from freshwater ecosystems in the Pampas region of Argentina: legacy and current use chemicals contribution. *Sci. Total Environ.* 691, 476–482. <https://doi.org/10.1016/j.scitotenv.2019.07.044>.

Johnson, R.L., Schmidt-Rohr, K., 2014. Quantitative solid-state ¹³C NMR with signal enhancement by multiple cross polarization. *J. Magn. Reson.* 239, 44–49. <https://doi.org/10.1016/j.jmr.2013.11.009>.

Khairiy, M.A., Luek, J.L., Dickhut, R., Lohmann, R., 2016. Levels, sources and chemical fate of persistent organic pollutants in the atmosphere and snow along the Western Antarctic Peninsula. *Environ. Pollut.* 216, 304–313. <https://doi.org/10.1016/j.envpol.2016.05.092>.

Kipka, U., Toro, D.M.D., 2011. A linear solvation energy relationship model of organic chemical partitioning to dissolved organic carbon. *Environ. Toxicology and Chemistry* 30 (9), 2023–2029. <https://doi.org/10.1002/etc.610>.

Lam, B., Simpson, A.J., 2008. Direct ¹H NMR spectroscopy of dissolved organic matter in natural waters. *Analyst* 133 (2), 263–269. <https://doi.org/10.1039/B713457F>.

Liu, K., Fu, H., Zhu, D., Qu, X., 2019. Prediction of apolar compound sorption to aquatic natural organic matter accounting for natural organic matter hydrophobicity using aqueous two-phase systems. *Environ. Sci. Technol.* 53 (14), 8127–8135. <https://doi.org/10.1021/acs.est.9b00529>.

Liu, K., Kong, L., Wang, J., Cui, H., Fu, H., Qu, X., 2020. Two-phase system model to assess hydrophobic organic compound sorption to dissolved organic matter. *Environ. Sci. Technol.* 54 (19), 12173–12180. <https://doi.org/10.1021/acs.est.0c03786>.

McKnight, D.M., Boyer, E.W., Westerhoff, P.K., Doran, P.T., Kulbe, T., Andersen, D.T., 2001. Spectrofluorometric characterization of dissolved organic matter for indication of precursor organic material and aromaticity. *Limnol. Oceanogr.* 46 (1), 38–48. <https://doi.org/10.4319/lo.2001.46.1.00038>.

Michaelson, G.J., Ping, C.L., Kling, G.W., Hobbie, J.E., 1998. The character and bioactivity of dissolved organic matter at thaw and in the spring runoff waters of the Arctic Tundra North Slope, Alaska. *J. Geophys. Res. Atmos.* 103 (D22), 28939–28946. <https://doi.org/10.1029/98JD02650>.

Miller, P.L., Chin, Y.P., 2002. Photoinduced degradation of carbaryl in a wetland surface water. *J. Agric. Food Chem.* 50 (23), 6758–6765. <https://doi.org/10.1021/jf025545m>.

Neale, P.A., Antony, A., Gernjak, W., Leslie, G., Escher, B., 2011. Natural versus wastewater derived dissolved organic carbon: implications for the environmental fate of organic micropollutants. *Water Res.* 45, 4227–4237. <https://doi.org/10.1016/j.watres.2011.05.038>.

Parnis, J.M., Mackay, D., 2020. *Multimedia Environmental Models: The Fugacity Approach*. CRC Press, Boca Raton, p. 301. ISBN 978-0367407827.

Peña, A., Rodríguez-Liébana, J.A., Delgado-Moreno, L., Rodríguez-Cruz, M.S., Sánchez-Martín, M.J., 2022. An overview of recent research on the role of dissolved organic matter on the environmental fate of pesticides in soils. *Pesticides in Soils: Occurrence, Fate, Control and Remediation*. Springer International Publishing, Cham, pp. 35–79. https://doi.org/10.1007/978-3-030-9698_2021_801. The Handbook of Environmental Chemistry.

Stenzel, A., Goss, K.U., Endo, S., 2013. Experimental determination of polyparameter linear free energy relationship (Pp-LFER) substance descriptors for pesticides and other contaminants: new measurements and recommendations. *Environ. Sci. Technol.* 47 (24), 14204–14214. <https://doi.org/10.1021/es404150e>.

Uhle, M.E., Chin, Y.P., Aiken, G.R., McKnight, D.M., 1999. Binding of polychlorinated biphenyls to aquatic humic substances: the role of substrate and sorbate properties on partitioning. *Environ. Sci. Technol.* 33 (16), 2715–2718. <https://doi.org/10.1021/es9808447>.

Vitale, C.M., Di Guardo, A., 2019. A review of the predictive models estimating association of neutral and ionizable organic chemicals with dissolved organic carbon. *Sci. Total Environ.* 666, 1022–1032. <https://doi.org/10.1016/j.scitotenv.2019.02.340>.

Ward, C., Cory, R., 2020. Assessing the prevalence, products, and pathways of dissolved organic matter partial photo-oxidation in arctic surface waters. *Environ. Sci. Processes Impacts* 22 (5), 1214–1223. <https://doi.org/10.1039/C9EM00504H>.

Wei-Haas, M.L., Hageman, K.J., Chin, Y.P., 2014. Partitioning of polybrominated diphenyl ethers to dissolved organic matter isolated from Arctic surface waters. *Environ. Sci. Technol.* 48 (9), 4852–4859. <https://doi.org/10.1021/es405453m>.

Weishaar, J.L., Aiken, G.R., Bergamaschi, B.A., Fram, M.S., Fujii, R., Mopper, K., 2003. Evaluation of specific ultraviolet absorbance as an indicator of the chemical composition and reactivity of dissolved organic carbon. *Environ. Sci. Technol.* 37 (20), 4702–4708. <https://doi.org/10.1021/es030360x>.

Wenk, J., Canonica, S., 2012. Phenolic antioxidants inhibit the triplet-induced transformation of anilines and sulfonamide antibiotics in aqueous solution. *Environ. Sci. Technol.* 46 (10), 5455–5462. <https://doi.org/10.1021/es300485u>.

Yang, X., Rosario-Ortiz, F.L., Lei, Y., Pan, Y., Lei, X., Westerhoff, P., 2022. Multiple roles of dissolved organic matter in advanced oxidation processes. *Environ. Sci. Technol.* 56, 1111–11131. <https://doi.org/10.1021/acs.est.2c01017>.